

# The SUNBIRD Survey: Insights into small-scale star formation mechanisms through near-infrared study of Young Massive Clusters

Zara Randriamanakoto<sup>1</sup> , P. Väisänen<sup>1,2</sup> and P. Ranaivomanana<sup>3</sup>

<sup>1</sup>South African Astronomical Observatory  
P.O. Box 9, Observatory 7935, South Africa  
email: [zara@sao.ac.za](mailto:zara@sao.ac.za)

<sup>2</sup>Southern African Large Telescope  
P.O. Box 9, Observatory 7935, South Africa

<sup>3</sup>Department of Astrophysics/IMAPP, Radboud Observatory  
P.O. Box 9010, 6500 GL, Nijmegen, The Netherlands

**Abstract.** We draw the  $K$ -band luminosity functions (CLFs) of young massive clusters (YMCs) hosted by 34 SUNBIRD targets to evaluate the impact of the host galaxy environment on their YMC properties. The depth and high resolution of the NIR images (PSF  $\sim 0.1''$ ) allow us to test whether CLF power-law slopes ( $\alpha$ ) of high star-forming galaxies are similar to those of gas-poor low star formation rate (SFR) galaxies. We found that  $\alpha$  ranges between 1.53 and 2.41 with a median value of  $1.87 \pm 0.23$ . We also performed correlation searches between  $\alpha$  and the host global properties and noticed that  $\alpha$  decreases with an increasing SFR and SFR density. On sub-galactic scales, CLF slopes of cluster-rich galaxies differ by  $\sim 0.5$ . Our NIR CLF analyses suggest that the extreme environment of high SFR galaxies such as the SUNBIRD sample is likely to affect the formation mechanisms of YMCs and hence to govern the ongoing small-scale SF processes of the host galaxy.

**Keywords.** galaxies: interactions, galaxies: star clusters, infrared: galaxies

---

## 1. Introduction

Young massive star clusters (YMCs) are usually found in large quantity in high star formation rate (SFR) galaxies such as interacting starburst galaxies ( $10.6 \lesssim \log(L_{\text{IR}}/L_{\odot}) < 11$ ) and luminous infrared galaxies (LIRGs,  $11 \lesssim \log(L_{\text{IR}}/L_{\odot}) < 12$ ). Low SFR galaxies such as normal spiral galaxies, nearby dwarf galaxies and circumnuclear rings of otherwise unremarkable galaxies are also known to host these young and compact objects. With their masses as massive as  $10^4 - 10^8 M_{\odot}$ , they represent the most massive and extreme form of star formation (SF) activity in galaxies (e.g. [Efremov 1995](#); [Randriamanakoto et al. 2019](#)). These make them good tracers of small-scale SF mechanisms. And since their properties are similar to those of global clusters (GCs) in terms of mass and density, they are also thought to be young GCs that are still forming today (see e.g. [Bastian 2016](#) for a review). Still embedded in their dust cocoons, YMC formation mechanisms, however, are not fully understood and hence deserve a more comprehensive investigation. One hot topic in this research area is whether the host environments influence the formation and evolution mechanisms of their cluster population. It is therefore

relevant to use near-infrared (NIR) observations which can probe deeper into the galaxy dusty nuclear regions, believed to be the nurseries of the most massive YMC candidates (Pflamm-Altenburg et al. 2013; Adamo et al. 2017; Randriamanakoto et al. 2019).

A pilot study by Randriamanakoto et al. (2013b) considered a representative sample of 8 local LIRGs with high SFRs observed with NIR adaptive optics (AO) instruments to construct the  $K$ -band cluster luminosity functions (CLFs,  $dN/dL \propto L^{-\alpha}$ ) of the targets. The intrinsic shape and power-law slope  $\alpha$  of the CLF are usually interpreted, not only because the CLF could be a mere reflection of the cluster initial mass function but also to help define a first order approximation of how the host environment affects the YMC physical and photometric properties. Randriamanakoto et al. (2013b) found that LIRGs have shallower slopes ( $\alpha \approx 1.9$ ) compared to those of gas-poor galaxies. This discrepancy is probably due to resolution bias and simple statistics (e.g. Whitmore et al. 2014; Mulia et al. 2016) and/or external factors such as the extreme environments of interacting LIRGs (e.g. Cook et al. 2016; Larson et al. 2020). We note however that no firm conclusions could not be drawn from this pilot study given the small sample size used in the work.

## 2. The SUNBIRD sample and the cluster catalogues

The local LIRGs studied by Randriamanakoto et al. (2013b) are part of the SUNBIRD survey (SUPERNOVAE and starBURSTS in the INFRARED or SUPERNOVAE UNMASKED BY INFRARED DETECTION, Väisänen et al. 2014; Kool et al. 2018). This NIR survey is an ongoing project mainly aimed at searching for optically hidden core collapse supernovae in the dusty regions of 42 starburst and luminous IR galaxies (Mattila et al. 2007; Kool et al. 2018). High spatial resolution instruments (PSF  $\sim 0.1''$ ) mounted on telescopes that are equipped with AO imaging (Gemini-N/ALTAIR/NIRI, Gemini-S/GeMS/GSAOI, VLT/NACO, and Keck II/NIRC2) were used to observe the  $K$ -band images of the targets. Other research projects focusing on the stellar population properties (Ramphul 2018) and the YMC populations (Randriamanakoto et al. 2013a,b) of the galaxy sample also used the SUNBIRD sample to probe further the physical details of SF activity in strongly star-forming galaxies.

By considering a larger sample of 34 targets from the SUNBIRD survey, the current work is a follow-up study of the pilot project done by Randriamanakoto et al. (2013b). Its goal is to deliver more robust  $K$ -band CLF analyses and thus contribute to addressing the differing views on the correlation between YMCs and their galaxy environments. The work is unique in a way that previous CLF works in the literature were mainly based either on optical observations (and hence miss the detection of highly embedded young YMCs) and/or on targets located less than  $\sim 20$  Mpc away to avoid dealing with resolution bias (but then exclude cluster-rich galaxies at larger distances). With a wide range of morphologies and interaction stages, the SUNBIRD targets studied in this work have an average SFR of  $\sim 30 M_{\odot} \text{ yr}^{-1}$  and luminosity distances  $D_L$  below 135 Mpc, except for IRAS 19115–2124 or the Bird where  $D_L \sim 206$  Mpc. We note that 8 of the 34 galaxies had their CLFs already published in the pilot study.

The same catalogues used by Randriamanakoto et al. (2013a) to establish the first ever relation between the NIR brightest cluster magnitude and the host's SFR are considered to build the CLFs in this work. A comprehensive description of the aperture photometry (with aperture radii of  $\sim 0.1''$ ) as well as the selection steps carried out to generate the final YMC catalogues can be found in Randriamanakoto et al. (2013b). The number of YMC candidates,  $N$ , in each catalogue ranges between 25 and 414. Targets with low number statistics of YMCs are not necessarily cluster-poor but their high inclination and/or a degraded AO correction are likely to challenge the extraction of these compact sources.

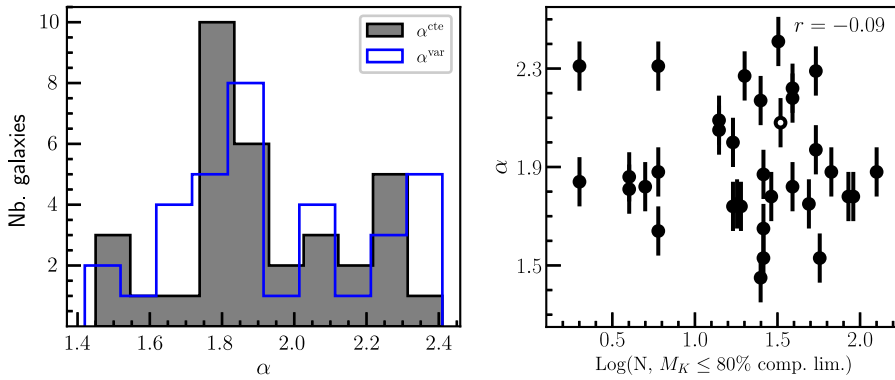


**Figure 1.** *Left:* Distributions of the power-law  $\alpha$  for the whole sample using a constant (cte, grey) and a variable binning (var, blue). The median values of  $\alpha$  are  $1.86 \pm 0.24$  and  $1.88 \pm 0.28$ , respectively. *Right:*  $\alpha^{\text{cte}}$  plotted against the number of YMCs with  $K$ -band magnitudes brighter than the 80 percent completeness level for each galaxy. The open circle denotes data points of the Bird.

### 3. The power-law slopes of the individual CLFs

Individual  $K$ -band CLFs of the 26 SUNBIRD targets (i.e. part of the sample not included in the pilot study) before and after completeness corrections were constructed using a constant and then a variable binning. We then fit a single power-law function to the corrected data until the 80 percent completeness level estimated from a Monte-Carlo (MC) completeness simulation. A constant binning of the CLFs results in  $1.53 < \alpha^{\text{cte}} < 2.41$  with a median and average values of  $\alpha_{\text{med}}^{\text{cte}} = 1.87 \pm 0.23$  and  $\alpha_{\text{aver}}^{\text{cte}} = 1.93 \pm 0.23$ , respectively. This range becomes  $1.42 < \alpha^{\text{var}} < 2.37$  in case of a variable binning, and with  $\alpha_{\text{med}}^{\text{var}} = 1.88 \pm 0.27$  and  $\alpha_{\text{aver}}^{\text{var}} = 1.94 \pm 0.27$ . The left panel of Fig. 1 compares the distributions of the power-law slopes derived from the two binning methods. The values of  $\alpha$  from the two methods are consistent within their uncertainties and they are also in agreement with the computed slopes in [Randriamanakoto et al. \(2013b\)](#) where  $\alpha \sim 1.9$ . Therefore, any observed flattening in the CLF could not be mainly due to the choice the binning. In the remainder of this work, we consider  $\alpha^{\text{cte}}$  from the constant binning, hereafter also referred to as the slope  $\alpha$ .

We also conducted other analyses to identify any possible uncertainties and biases and to test the robustness of our results. These include varying the PSF size of the MC completeness simulations, assessing the effects of resolution bias and extinction. In particular, we verified whether statistical bias and stochastic sampling strongly affect the CLFs of galaxies with low-number statistics of YMCs. The right panel of Fig. 1 plots the slope  $\alpha$  against  $\log N$ , which is the number of YMCs with magnitudes brighter than the 80 percent completeness limit in this case. With a correlation coefficient  $r = -0.09$ , there is no clear trend between the two entities. Overall, none of the various uncertainties and biases investigated in this work did not seem to have significantly flatten the CLFs of the YMC catalogues. What could then be the reason(s) behind a CLF slope smaller than the canonical value of  $\alpha \approx 2$ ?

### 4. Composite CLFs of supergalaxies split as a function of the host global properties

We also built CLFs from composite “supergalaxies” using a constant binning and corrected for observational completeness. The data are created by combining the individual catalogues in different ways with the aim to increase the number statistics of YMCs for more robust results. Data points from the Bird are not included in this analysis to avoid

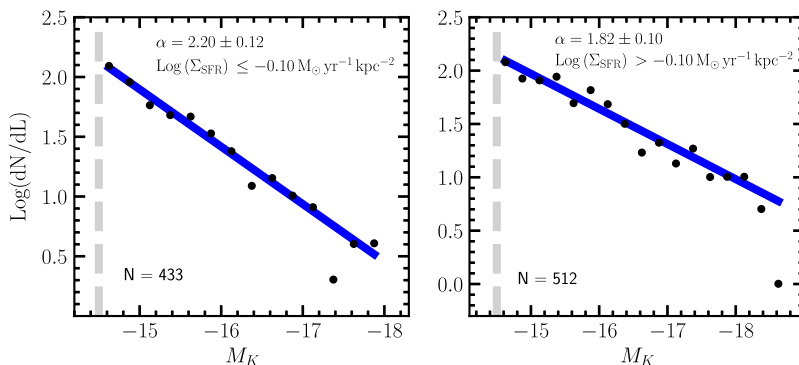


**Figure 2.** Completeness-corrected composite CLFs of the SUNBIRD targets with the individual star cluster catalogues (excluding the Bird) divided as a function of the host galaxy’s SFR density, below (*left*) and above (*right*)  $\log(\Sigma_{\text{SFR}}) = -0.10 \text{ M}_{\odot} \text{ yr}^{-1}$ . The vertical line denotes the 80 percent completeness level until which a single power-law function (blue line) is fitted to the corrected data. The number of YMCs considered in the fitting process along with the computed slopes are added as insets in the CLF plots.

bias. By combining the YMCs of 33 galaxies, the composite CLF which is fitted down to a magnitude limit  $M_K = -14.5$  mag, i.e. where 80 percent of the SUNBIRD data should be complete, has a bright end slope of  $\alpha = 1.98 \pm 0.10$ . This value is consistent with the average slope of the individual CLFs in Section 3.

#### 4.1. Sample split as a function of the SFR density

Among the composite CLFs of supergalaxies created in this work (e.g. based on the galaxy distances, SFR, specific SFR = SFR/Mass), we show in Fig. 2 the cases where the main sample is split with respect to the SFR density of the host galaxy:  $\log(\Sigma_{\text{SFR}}) \leq -0.10 \text{ M}_{\odot} \text{ yr}^{-1} \text{ kpc}^{-2}$  (left panel) and  $\log(\Sigma_{\text{SFR}}) > -0.10 \text{ M}_{\odot} \text{ yr}^{-1} \text{ kpc}^{-2}$  (right). This cutoff was chosen given that it is the average of the SFR density. The computed power-law slopes are  $\alpha = 2.20 \pm 0.12$  and  $\alpha = 1.82 \pm 0.10$ , respectively. The value of  $\alpha$  increases by  $\Delta\alpha = 0.38$  with a decreasing SFR density. Such trends were also observed while dividing the sample as a function of the SFR ( $\Delta\alpha \sim 0.44$  for a cutoff of  $\text{SFR} = 30 \text{ M}_{\odot} \text{ yr}^{-1}$ ) and the specific SFR ( $\Delta\alpha = 0.40$  for a cutoff of  $\log(\text{sSFR}) = 9.68 \text{ yr}^{-1}$ ). We note that host global properties used here and in Section 5 were mostly taken from Ramphul (2018).

#### 4.2. Composite CLFs of cluster-rich galaxies on sub-galactic scales

We also constructed composite CLFs of cluster-rich galaxies with  $N \gtrsim 300$  (IC 2522, ESO 221–IG008, NGC 3110, and NGC 6000). While the power-law CLF slope of such supergalaxy is  $\alpha = 2.18 \pm 0.09$ , the composite CLFs of two distinct subsamples segregated by the cluster physical locations in the field of the galaxy have slopes  $\alpha = 1.72 \pm 0.11$  for the nuclear regions and  $\alpha = 2.51 \pm 0.09$  for the arms or other starburst regions of the field.

This analysis on sub-galactic scales was also performed using the catalogues of each individual cluster-rich galaxy. Table 1 summarizes the computed values of  $\alpha$  for a nuclear (Col 8) vs outer (Col 10) regions assuming their respective completeness limits (Cols 7 & 9). CLF slopes of the nuclear regions are shallower compared to those of the outer regions for NGC 3110 and NGC 6000. Similar values are found for both regions of the other two galaxies. Table 1 lists as well the computed CLF slopes of the whole catalogue for each target while estimating the completeness limits based on the background contour levels (Col 3) and then the galaxy morphology (Col 5). The values of the two parameters remain

**Table 1.** The values of  $\alpha$  and the 80% completeness limits in various regions of cluster-rich galaxies.

Galaxy name	N	Contour levels		Galaxy morphology		Nuclear regions		Outer regions	
(1)	(2)	CL (3)	$\alpha_1$ (4)	CL (5)	$\alpha'_1$ (6)	CL (7)	$\alpha$ (8)	CL (9)	$\alpha$ (10)
IC 2522	302	-12.2	$2.41 \pm 0.08$	-12.2	$2.40 \pm 0.08$	-12.4	$2.55 \pm 0.19$	-12.2	$2.31 \pm 0.10$
ESO 221-IG008	414	-11.9	$2.00 \pm 0.11$	-11.7	$1.98 \pm 0.09$	-11.8	$2.06 \pm 0.11$	-12.1	$2.11 \pm 0.16$
NGC 3110	279	-13.8	$2.31 \pm 0.08$	-13.9	$2.25 \pm 0.07$	-14.5	$1.92 \pm 0.08$	-13.7	$2.43 \pm 0.09$
NGC 6000	285	-12.5	$1.82 \pm 0.19$	-12.3	$1.81 \pm 0.19$	-12.9	$1.44 \pm 0.07$	-12.3	$2.24 \pm 0.10$

Notes: The different regions and the corresponding 80% completeness limits (CLs) were defined based on the background contour levels and then considering the nuclear and outer regions of the galaxy.

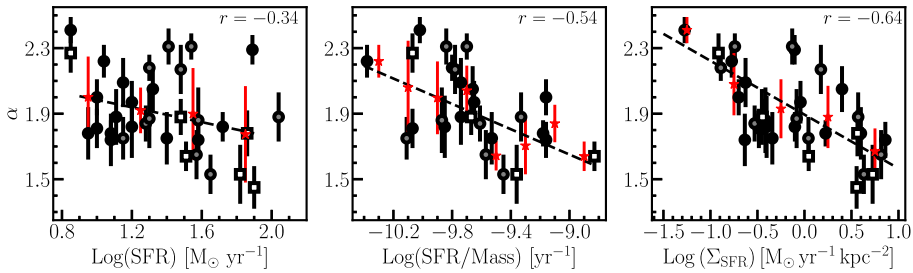


**Figure 3.** The power-law slope plotted against the host galaxy’s SFR (left), specific SFR (middle), and SFR density (right). The data points are labelled as a function of the host galaxy distance: black circles for  $D_L \leq 60$  Mpc, grey circles for  $60 < D_L \leq 100$  Mpc, and open squares for  $D_L > 100$  Mpc. Red stars represent derived data points from a constant binning of  $\alpha$  and the dashed line a linear fit to these data.

consistent within the error estimates which imply that using equally-spaced background levels to output the 80 percent completeness limits applied to the individual CLFs in Section 3 are reasonable.

### 5. Correlation searches between the host global properties

Correlation searches between  $\alpha$  and the host global properties were also conducted to check whether the trends seen in the composite CLFs on both global and sub-galactic scales are real. Fig. 3 shows in particular the trends with the galaxy’s SFR (left), specific SFR (middle), and SFR density (right). The values of the correlation coefficient are  $r = -0.34, -0.54, -0.64$ , respectively. These coefficients become  $r = -0.97, -0.86, -0.97$  once we bin the data points (red stars). These clearly indicate the existence of a (mild) correlation between  $\alpha$  and the three SFR indicators, with the strongest correlation associated with  $\alpha$  vs.  $\Sigma_{\text{SFR}}$  plot. Correlation searches with other global properties such as the stellar mass, the light-weighted metallicity, or the stellar visual extinction were also done but only very weak or no trend could only be observed.

### 6. Conclusions and way forward

This work summarizes major results from drawing the constructed  $K$ -band cluster luminosity functions of 34 SUNBIRD targets imaged with NIR AO telescopes (a comprehensive report on this research project is available in Randriamanakoto et al. 2022). These main findings are as follows: smaller values of the (median and average) slopes compared to the canonical index of  $\alpha \sim 2$ , a flattening CLF slope with an increasing SFR indicator (especially in the case of the SFR density), and the difference by  $> 0.4$  in the CLF slopes for individual cluster-rich catalogues and supergalaxies split as a function of the cluster physical locations or the host SFR, specific SFR, and SFR density.

We demonstrated that internal factors such as size-of-sample effects and other systematic biases cannot only explain the observed trends in this work. Previous works by e.g. Whitmore et al. (2014), Mulia et al. (2016), and Cook et al. (2019) merely associate similar trends to size-of-sample effects which they believe are the main responsible for any artificially flattened CLF. This also means that the cluster formation mechanisms generally remain the same irrespective of the host SFR level. However, other works that also recorded unusual YMC properties of high-star forming galaxies explain the observed trends as a consequence of some underlying process involving the host galaxy environment (e.g. Bastian et al. 2012; Cook et al. 2016; Randriamanakoto et al. 2019). For instance, environments with high gas surface density are generally of higher interstellar medium pressure and are thus ideal birthsites of strongly bound clusters such as YMCs (e.g. Kruijssen 2012; Espada et al. 2018).

Given that rigorous assessment of any possible biases have been conducted before interpreting our results, we are thus likely in favour of the latter explanation, i.e. the CLF and hence the cluster SF processes being influenced by its host environment. However, we are aware that CLFs can only provide first order approximation of the effects of internal and/or external factors on the cluster population and that this work has as well its own limitations (e.g. drawing binned CLFs, using a single filter or comparing our NIR-based results with optical CLF studies of low SFR galaxies). Therefore, further analyses need to be implemented such as the use of other fitting techniques that involve maximum-likelihood estimation of cumulative CLFs. Moreover, a comprehensive multi-wavelength study of the cluster population of the SUNBIRD targets will allow the modelling of the cluster ages and masses to provide better constraints of the cluster SF formation processes and ultimately the small-scale SF mechanisms of the host galaxy.

## Acknowledgements

ZR acknowledges funding from the South African Astronomical Observatory, which is a facility of the National Research Foundation, and financial support from the L'Oréal - UNESCO For Women In Science sub-Saharan Africa regional Programme.

## References

- Adamo, A., Ryon, J. E., Messa, M., et al. 2017, *ApJ*, 841, 131
- Bastian, N. 2016, *EAS Publications Series*, 80, 5
- Bastian, N., Adamo, A., Gieles, M., et al. 2012, *MNRAS*, 419, 2606
- Cook, D. O., Dale, D. A., Lee, J. C., et al. 2016, *MNRAS*, 462, 3766
- Cook, D. O., Lee, J. C., Adamo, A., et al. 2019, *MNRAS*, 484, 4897
- Efremov, Y. N. 1995, *AJ*, 110, 2757
- Espada, D., Martin, S., Verley, S., et al. 2018, *ApJ*, 866, 77
- Kool, E. C., Ryder, S., Kankare, E., et al. 2018, *MNRAS*, 473, 5641
- Kruijssen, J. M. D. 2012, *MNRAS*, 426, 3008
- Larson, K. L., Díaz-Santos, T., Armus, L., et al. 2020, *ApJ*, 888, 92
- Mattila, S., Väisänen, P., Farrah, D., et al. 2007, *ApJL*, 659, L9
- Mulia, A. J., Chandar, R., & Whitmore, B. C. 2016, *ApJ*, 826, 32
- Pflamm-Altenburg, J., González-Lópezlira, R. A., & Kroupa, P. 2013, *MNRAS*, 435, 2604
- Ramphul, R. 2018, PhD thesis, Department of Astronomy, University of Cape Town, South Africa
- Randriamanakoto, Z., Escala, A., Väisänen, P., et al. 2013a, *ApJL*, 775, L38
- Randriamanakoto, Z., Väisänen, P., Ranaivomanana, P., et al. 2022, *MNRAS*, 513, 4232
- Randriamanakoto, Z., Väisänen, P., Ryder, S. D., et al. 2013b, *MNRAS*, 431, 554
- Randriamanakoto, Z., Väisänen, P., Ryder, S. D., et al. 2019, *MNRAS*, 482, 2530
- Väisänen, P., Randriamanakoto, Z., Escala, A., et al. 2014, *Massive Young Star Clusters Near and Far: From the Milky Way to Reionization*, p. 185
- Whitmore, B. C., Chandar, R., Bowers, A. S., et al. 2014, *AJ*, 147, 78